Table S1 | Data collection and refinement statistics

	Nurr1-NBRE
PDB entry	7WNH
Data collection	SSRF BL19U1
Wavelength (Å)	0.97775
Space group	$P3_2$
Unit cell (Å, °)	$a = b$=124.0, c= 119.5
Molecules per asymmetric unit	4
Resolution range (Å) [a]	119.52-3.10（3.24-3.10）
Unique reflections	37212
Completeness (%)	99.7 (99.9)
$<I/\sigma(I)>$	7.9 (1.8)
R_{pim} [b] (%)	5.6 (37.9)
Average redundancy	9.6 (9.7)
Refinement statistics	
Resolution range (Å)	107.39-3.10
R-factor[c]/R-free[d] (%)	22.3/26.7
RMSD[e] bond lengths (Å)	0.007
RMSD bond angles (°)	1.449
Mean B factor (Å^2)	
protein	91.4
DNA	88.4
water	51.0
Ramachandran plot	
Most favored (%)	91.7
Additional allowed (%)	7.7
Outlier	0.6

[a] The values in parentheses refer to statistics in the highest resolution bin.

[b] R_{pim} is the precision-indication merging R factor.

[c] R-factor =$\sum_h$|Fo(h) - Fc(h)|/ $\sum_h$Fo(h), where Fo and Fc are the observed and calculated structure-factor amplitudes, respectively.

[d] R-free was calculated with randomly excluded 5% of data.

[e] Root-mean square-deviation from ideal values.

Table S2 | SAXS sample details and parameters

Data Collection Parameters		
SEC-SAXS column		Superdex 200 Increase 10/300GL
Loading concentration		7 mg/mL
Flow rate		0.3 mL/min
Solvent		20 mM Tris-HCl, pH7.5, 150 mM NaCl
Structural Parameters		
From Guinier fit	I(0) (cm^{-1})	0.025±0.00014
	Rg (Å)	33.51±0.27
From *P*(*r*)	I(0) (cm^{-1})	0.2548E-01±0.9566E-04
	Rg (Å)	34.42±0.03
	Dmax (Å)	98.74
Molecular Mass Determination		
MM (kDa) from Q(p)		44.105
MM (kDa) from V(c)		39.01
Estimate MW (kDa)		42.85
Modeling		
DAMMIN	χ^2	1.061
	NSD	1.054±0.087
	Ensemble Resolution	41±3
CRYSOL	χ^2	1.9

Table S3. The interfaces Edges of Nurr1-RXRα model

Nurr1-LBD	RXRα-LBD	Nurr1-DBD	RXRα-DBD	Nurr1-LBD	RXRα-DBD	Nurr1-DBD	RXRα-LBD
T513	L420	Y297	N174	N542	L178	P306	A387
E514	K417	R310	E219	N543	D176	R310	E388
E514	L420	R312	T170	G545	A197	R311	E388
E514	R421	N313	T170	L546	K194		
Q528	G413	N313	C171	L546	A197		
N529	P412	R314	N174	L546	M198		
V532	P412	R314	K175	N547	K175		
N550	E394	R314	S129	N547	D176		
N550	V396	C315	N174	N547	C177		
S553	Y397	Q316	N174	N547	Q193		
S553	A398	R341	D173	R548	K175		
S553	E401	R341	N174	P549	Q193		
S553	F415	R341	D176	P549	A197		
K554	E394	G343	D176				
L556	F415	R344	D176				
L556	L419	P358	M198				
G557	Y397						
G557	L419						
L559	A416						
L559	L420						
P560	L419						
P560	P423						
R563	L420						
R563	P423						
T564	P423						

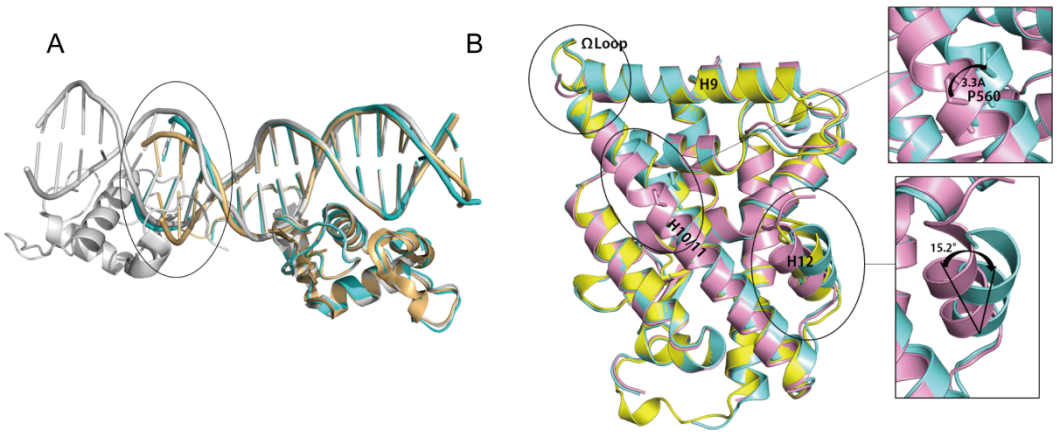

Fig. S1 | Superposition analysis of Nurr1-NBRE structure (A) Superposition of Nurr1 DBD binding with NBRE (cyan), rat NGFI-B (light orange, PDB: 1CIT) and Nurr1 DBD binding with inverted repeat element (grey, PDB: 6L6Q). (B) Superposition of LBD in Nurr1258-NBRE (aquamarine, chain D, pink, chain C) and previously reported apo Nurr1 LBD (yellow, PDB:1OVL (11)).

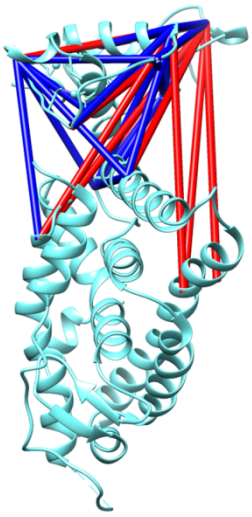

Fig. S2 | High-confidence crosslinks of Nurr1 without DNA binding were labeled on Form 1. Dark bule for the satisfied crosslinks and red for the violated ones.

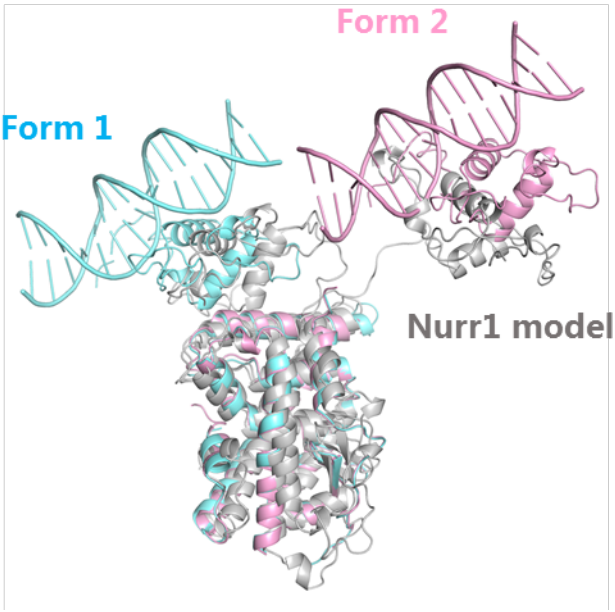

Fig. S3 | MD analysis of Nurr1 monomer structure. Models (grey) identified in MD trajectories starting from the $Nurr1_{258}$ Form 1 are similar to the two Nurr1 structures, Form 1 (aquamarine) and Form 2 (pink).

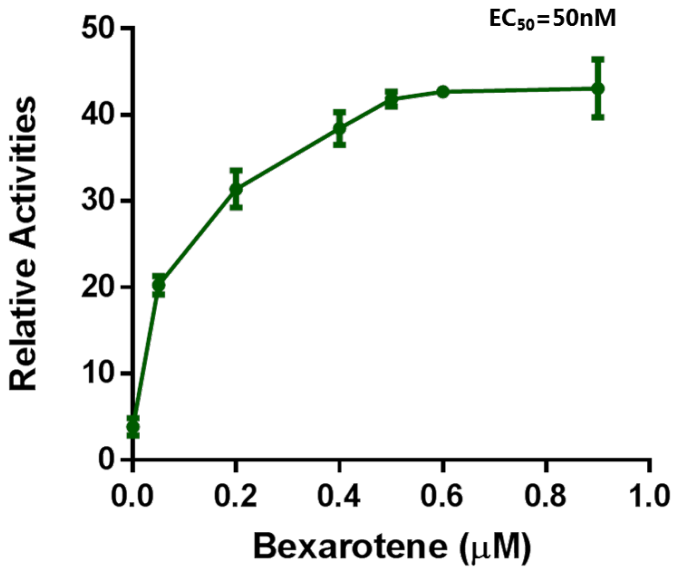

Fig. S4 | Does-response of Bexarotene on the transcription activity. The EC_{50} of Bexarotene was measured in 293T cells co-transfected with IR5-driven luciferase reporter plasmid and full-length Nurr1 and RXRα plasmids.

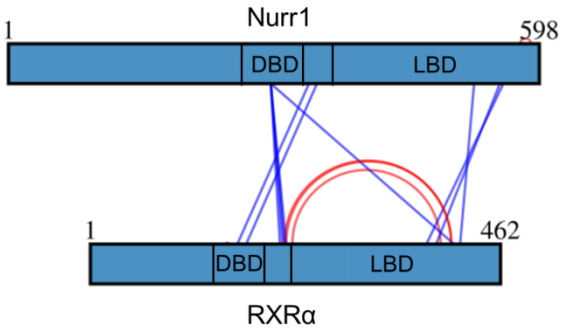

Fig. S5 | Map of high-confidence EDC crosslinked residues shown schematically on the Nurr1 and RXRα. Dark blue lines connected the intermolecular crosslinked peptides; red arc connected the intramolecular crosslinked peptides.

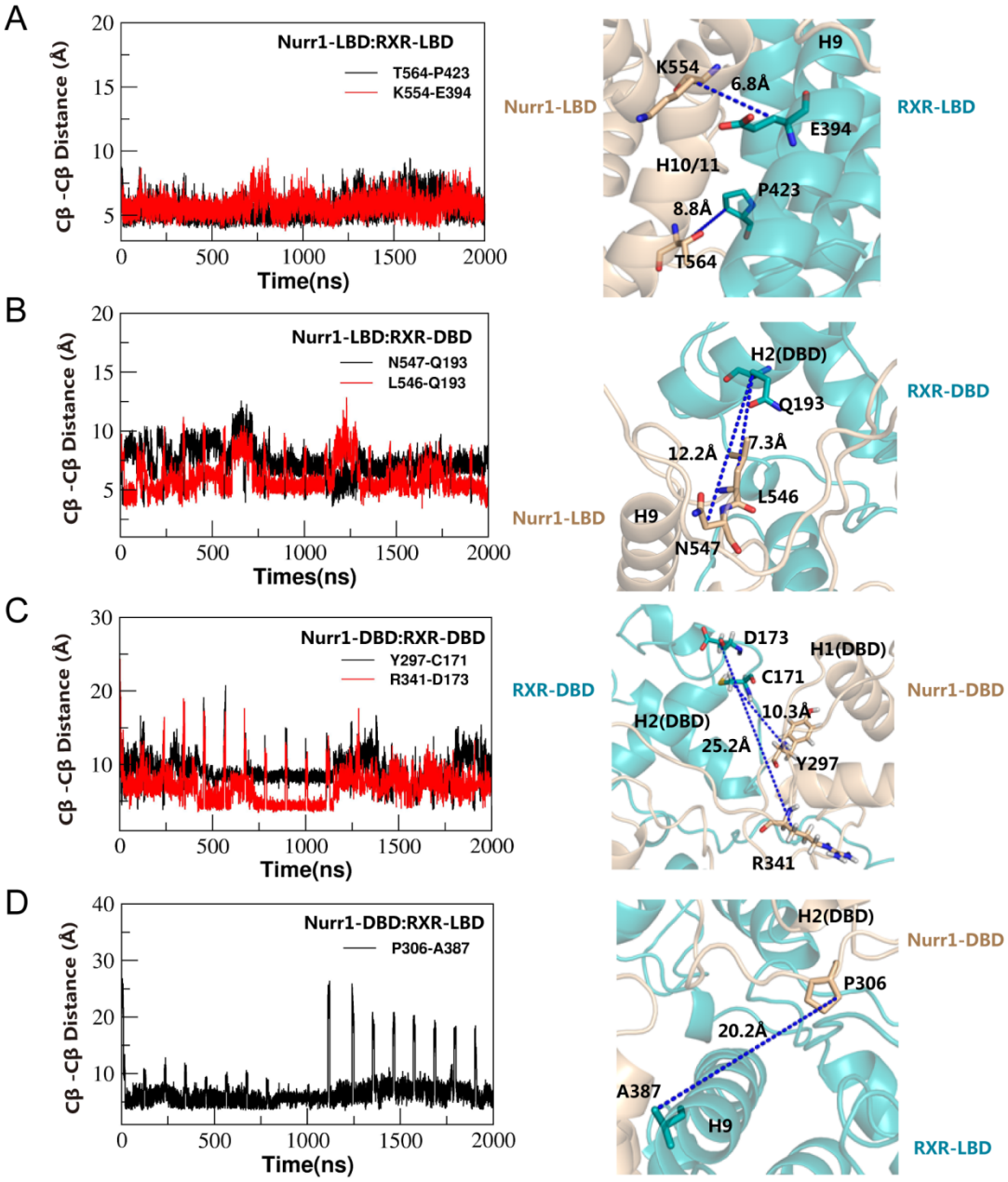

Fig. S6 | Analysis of the inter-domain contacts in the Nurr1-RXRα Model. Cβ atom distances of residue pairs from inter-domain interfaces during MD simulation of the Nurr1-RXRα heterodimer model (left panel) and distances measured from the model (right panel), (A) Nurr1-LBD: RXRα-LBD interface. (B) Nurr1-LBD: RXRα-DBD interface. (C) Nurr1-DBD: RXRα-DBD interface. (D) Nurr1-DBD: RXRα-LBD interface.

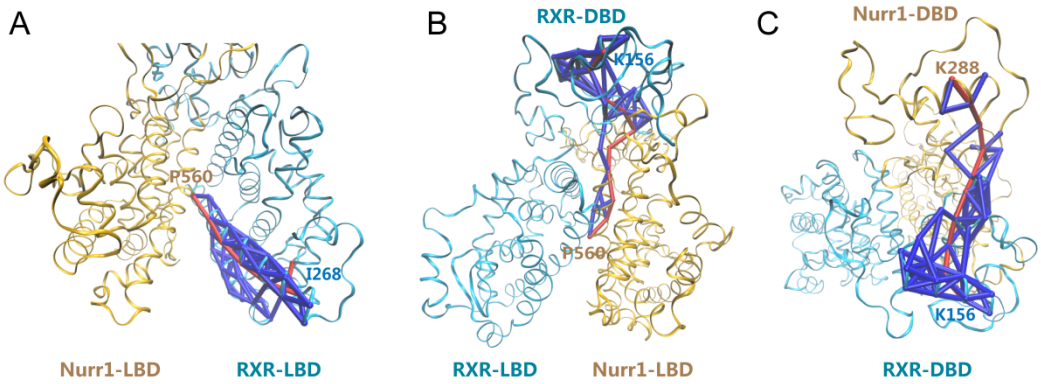

Fig. S7 | Optimal and suboptimal path analysis reveals coupling routes between Nurr1 and RXRα. (A) Nurr1-LBD and RXRα-LBD. (B) Nurr1-LBD and RXRα-DBD. (C) Nurr1-DBD and RXRα-DBD. Optimal paths were highlight by red and suboptimal paths were colored blue. The source and sink nodes of Nurr1 and RXRα were labeled.

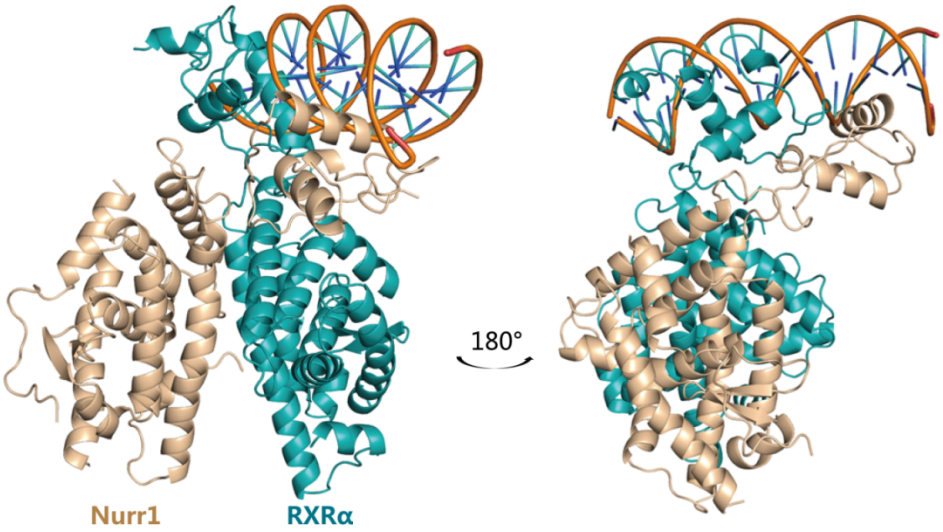

Fig. S8 | Nurr1-RXRα-IR5 model generated by Paradock. Nurr1, wheat; RXRα, teal; IR5, orange.

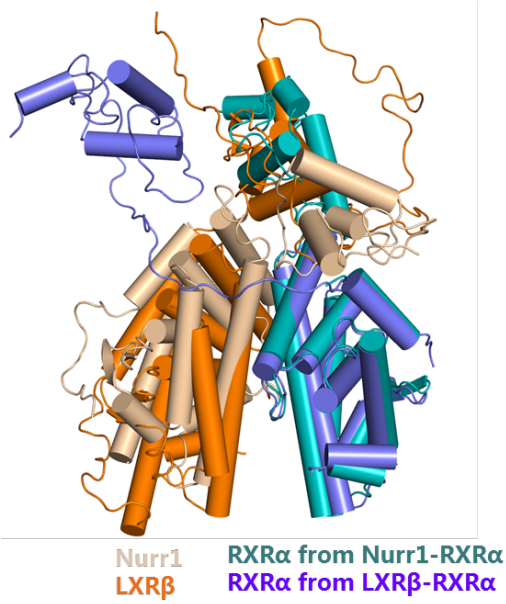

Fig. S9 | Superposition of LXRβ-RXRα and Nurr1-RXRα model. Nurr1(wheat), LXRβ(orange), RXRα of Nurr1-RXRα (teal), RXRα of LXRβ-RXRα (purple).

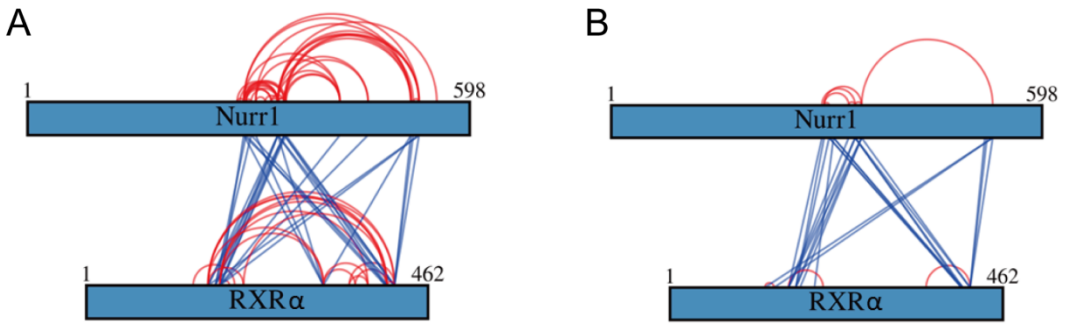

Fig. S10 | Map of high-confidence BS3 crosslinked residues shown schematically on the Nurr1 and RXRα sequence, dark blue lines connected the intermolecular crosslinked peptides, red arc connected the intramolecular crosslinked peptides. (A) Crosslinking sample of Nurr1-RXRα heterodimer without Bexarotene. (B) Crosslinking sample of Nurr1-RXRα heterodimer incubated with Bexarotene.